Carbohydrate Research 345 (2010) 1760–1766

Contents lists available at ScienceDirect

Carbohydrate Research

journal homepage: www.elsevier.com/locate/carres

Dynamic stereochemistry of rutin (vitamin P) in solution: theoretical approaches and experimental validation

Mina Ghiasi [a,*], Salman Taheri [b], Mohsen Tafazzoli [b]

[a] Department of Chemistry, Faculty of Science, Alzzahra University, PO Box 19835-389, Vanak, Tehran, Iran
[b] Department of Chemistry, Sharif University of Technology, PO Box 11365-9516, Tehran, Iran

ARTICLE INFO

Article history:
Received 8 February 2010
Received in revised form 11 May 2010
Accepted 13 May 2010
Available online 24 May 2010

Keywords:
Rutin
Karplus equation
Coupling constants
^{1}H–^{1}H COSY
HMQC
HMBC

ABSTRACT

Rutin, vitamin P, was extracted from *Salvia macrosiphon* and identified by ^{1}H, ^{13}C, ^{1}H–^{1}H COSY, HMQC, and HMBC spectroscopy. In parallel, density functional theory (DFT) using B_3LYP functional and split-valance 6-311G** basis set has been used to optimize the structures and conformers of rutin. Also experimental and theoretical methods have been used to correlate the dependencies of ^1J, ^2J, and ^3J involving ^{1}H and ^{13}C on the C5″–C6″ (ω), C6″–O6″ (θ), and C1‴–O6″ (φ) torsion angles in the glycosidic moiety. New Karplus equations are proposed to assist in the structural interpretation of these couplings. $^3J_{HH}$ depends mainly on the C–C (ω) torsion angle, as expected, and $^2J_{HH}$ values depend on both C–C (ω) and C–O (θ) torsions. $^1J_{CH}$ values within hydroxymethyl fragments were also examined and found to depend on r_{CH}, which is modulated by specific bond orientation and stereoelectronic factors. In all calculations solvent effects were considered using a polarized continuum model (PCM).

1. Introduction

Bioflavonoids are benzo-γ-pyrone derivatives of plant origin with a wide range of physiological activities such as antioxidant, antimicrobial, anti-inflammatory, antiallergenic, antiviral, and anti-tumor properties.[1–4] Rutin (Fig. 1) is a non-toxic bioflavonoid composed of the flavonol quercetin and the disaccharide rutinose that is found in more than 70 plant species. It is used clinically in therapeutic medicine,[5,6] especially in humans for the treatment of lymphoedema following axillary lymph node excision.[7] It has less toxicity in the human body and has the potential to be a novel therapeutic agent.

Some analytical methods, including capillary electrophoresis,[8] cyclic voltammetry,[9] HPLC,[10] chemiluminescence,[11] electrochemical sensor,[12] spectrophotometry,[13] and sequential injection analysis,[14] have been applied to the determination of the structure and properties of rutin, but it is still necessary to develop methods to quantify rutin in pharmaceutical preparations or crude drugs.

Recently the interaction of rutin with some flavonoids with DNA has been studied, but how flavonoid molecules bind to DNA is currently unclear. The function of the glycosidic ring, for example, is not understood.[15–17] In this study we focused on the sugar chain of rutin (rutinose) to determine its conformation in solution.

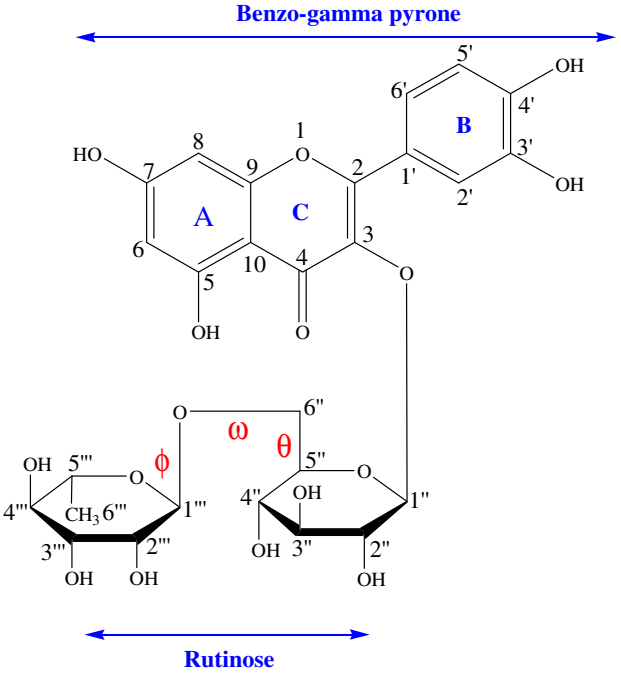

Figure 1. Chemical structure of rutin.

* Corresponding author. Tel.: +98 2188044051–9x2608; fax: +98 2188041344.
E-mail address: ghiasi@alzahra.ac.ir (M. Ghiasi).

0008-6215/$ - see front matter © 2010 Elsevier Ltd. All rights reserved.
doi:10.1016/j.carres.2010.05.013

Determination of the conformation of biologically active molecules is often based on NMR spectral data in combination with computational methods. In the present work, we are interested in extending the use of *J*-coupling constants for the structural, stereochemical, and conformational analysis of vitamin P by definition of the dependences of $^{3}J_{HH}$, $^{2}J_{HH}$, and $^{1}J_{CH}$ coupling constants on the $^{1}H/^{13}C$ atomic dihedral angles in the sugar chain. So we present the results of studies of chemical shifts and a set of *J*-couplings about the C5″–C6″ (ω), C6″–O6″ (θ), and C1‴–O6″ (φ) bonds, $^{3}J_{HH}$, $^{2}J_{HH}$, and $^{1}J_{CH}$, on rutinose, using experimental and theoretical methods to determine the Karplus equation.

2. Experimental

2.1. Extraction and separation

The air-dried and powdered aerial parts of wild (960 g) *Salvia macrosiphon* were defatted with hexane and extracted with 90% EtOH (3 × 3 L) at room temperature for six days. The combined extracts were concentrated, and the residue (30 g) was dissolved in H_2O (600 mL) and extracted with EtOAc (3 × 50 mL). The EtOAc-soluble part was subjected to column chromatography over silica gel (E. Merck, 70–230 mesh) and eluted with $CHCl_3$, $CHCl_3$–EtOAc, EtOAc, and 9:1–1:1 EtOAc–MeOH. Concentration of the 1:1 EtOAc–MeOH fractions afforded a yellow residue (0.11 g), which on purification by preparative paper chromatography using 4:1:5 *n*-BuOH–HOAc (40–10%)–H_2O gave rutin (15 mg). The UV–vis spectrum of rutin in methanol solvent shows three peaks at 220 nm, 255 nm, and 371 nm (λ_{max}).

2.2. NMR measurements

^{1}H NMR, ^{13}C NMR, DEPT, ^{1}H–^{1}H COSY, HMQC, and HMBC spectra of rutin were taken at 298 K in DMSO (99.99% D) on a Bruker Avance DRX operating at 500.133 MHz for ^{1}H and 125.770 MHz for ^{13}C, using a 5-mm broad band inverse probe with sufficient digital resolution to ensure errors ⩽0.1 Hz in the measured *J*-couplings.

All 2D NMR spectra were acquired by pulsed field gradient-selected methods. 2D correlation spectroscopy (COSY) was used to confirm ^{1}H assignments. Heteronuclear multiple quantum correlation (HMQC) and heteronuclear multiple bond correlation (HMBC) were used for ^{13}C assignments.

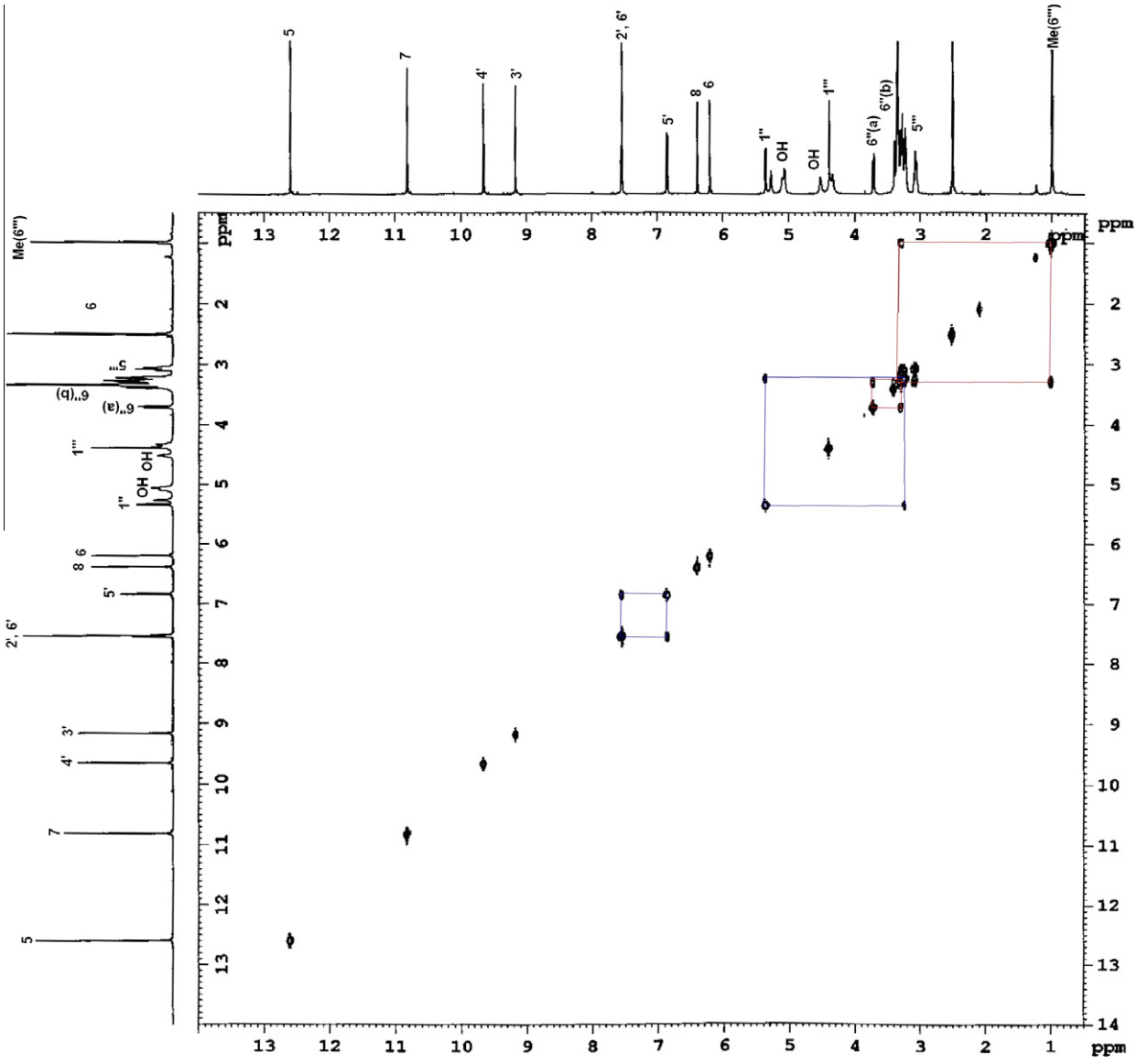

Figure 2. ^{1}H–^{1}H COSY spectrum of rutin in DMSO-d_6 at 298 K.

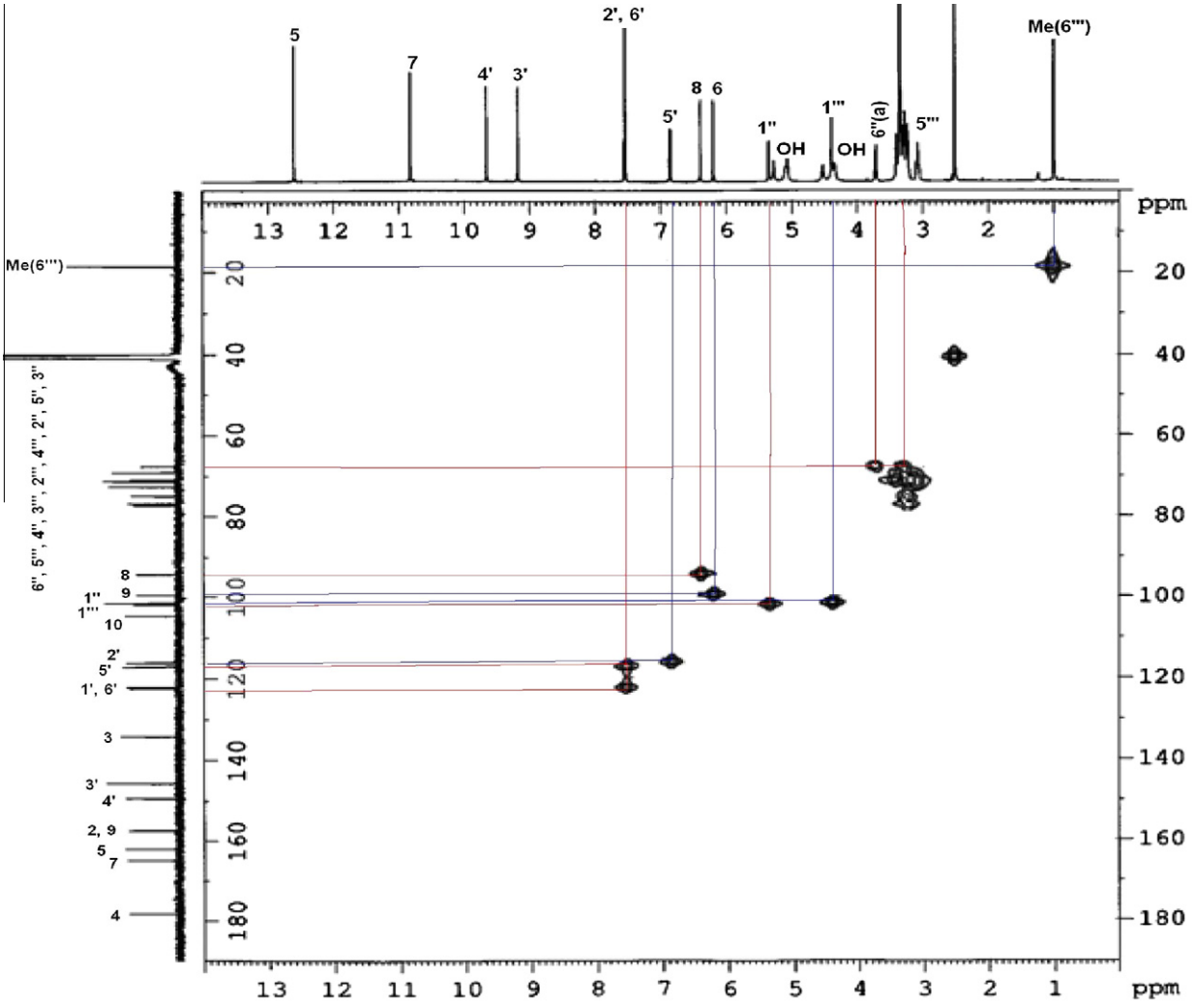

Figure 3. HMQC spectrum of rutin in DMSO-d_6 at 298 K.

Figures 2–4 show the ^{1}H–^{1}H COSY, HMQC, and HMBC spectra of rutin, respectively, and the ^{13}C NMR of extracted rutin is in good agreement with that reported in the literature.[18]

HMQC and HMBC spectra were recorded using 2048 × 1024 data matrices; the number of scan and dummy scans were 48 and 16, respectively, in all cases.

The HMQC and HMBC spectra were recorded with 2 s interpulse delay. The spectral widths $sw_1 \times sw_2$ = 3255 × 22,123 Hz in all 2D experiments. For *Z*-only gradients, the *G*1:*G*2:*G*3 = 50:30:40.1 gradient ratios were used for both the HMQC and the HMBC spectra.

3. Computational details

3.1. Ab initio molecular orbital calculation

Ab initio calculations were carried out with the GAUSSIAN program series 2003.[19] The optimization of the geometry was performed employing a hybrid Hartree–Fock density-functional scheme, the adiabatic connection method, that is, the Becke three-parameter with Lee–Yang–Parr (B_3LYP) functional of density functional theory (DFT)[20] with the standard basis set, 6-311G**. Full optimizations were performed without any symmetry constraints. We computed the harmonic vibrational frequencies to confirm that an optimized geometry correctly corresponds to a local minimum that has only real frequencies. The solvent effects on the conformational equilibrium have been investigated with a PCM method[21] at the B_3LYP/6-311G** level. Solvation calculations were carried out for DMSO (ε = 46.7) with the geometry optimization for this solvent. Conformational energy profiles around the C5″–C6″ and C1‴–O6″ bond in rutinose, Figure 5, were calculated by driving the ω and θ dihedral angles from 0° to 360° in 30° increments, while allowing the remaining geometrical parameters to relax. In this report the orientations about the C5″–C6″, C6″–O6″, and C1‴–O6″ are described by torsion angles (ω = O5″–C5″–C6″–O6″), (θ = C5″–C6″–O6″–C1‴), and (φ = H1‴–C1‴–O6″–C6″). For the C5″–C6″ and C1‴–O6″ rotamers we used the standard nomenclature, Scheme 1. The O5″ and C4″ are the reference atoms and staggered conformers are designated as the *gt* ($\omega \approx 60$), *tg* ($\omega \approx 180$), and *gg* ($\omega \approx -60$).

4. Results and discussion

4.1. Geometry optimization of rutin

The rutin structure was fully optimized by the B_3LYP method using the 6-311G** basis set with no initial symmetry restrictions and assuming a C_1 point group. The optimized geometry of rutin in the gas phase was reoptimized by considering the solvent effect (ε = 46.7) using the polarized continuum model (PCM). Tomasi's polarized continuum model defines the cavity as the union of a ser-

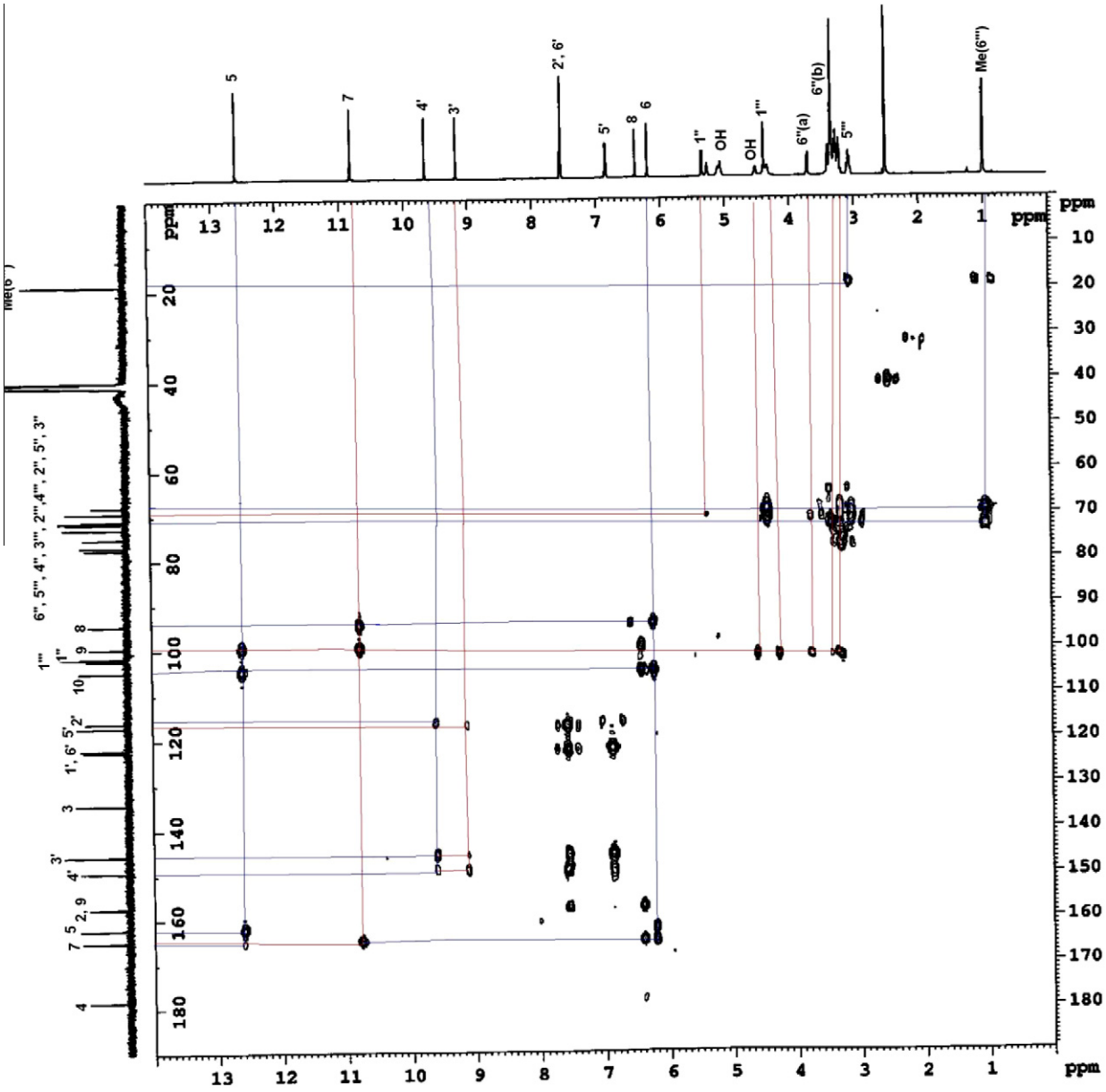

Figure 4. HMBC spectrum of rutin in DMSO-d_6 at 298 K.

ies of interlocking atomic spheres. The effect of polarization of the solvent continuum is represented numerically.[21] Figure 5 shows the optimized structure of rutin in DMSO solvent.

A selection of calculated bond distances, bond angles, and dihedral angles are compiled in Table 1. Calculation of vibrational frequencies has confirmed a stationary point with no negative eigenvalue observed in the force constant matrix.

4.2. Calculation of chemical shifts and NMR spin–spin coupling constants

NMR computations of absolute shieldings were performed using the GIAO method[22] on the DFT-optimized structure in the presence of solvent. The ^{1}H and ^{13}C chemical shifts were calculated by using the corresponding absolute shieldings calculated for Me_4Si at the same level of theory (Table 2). A good agreement between the experimental and theoretical chemical shifts shows the reliability of DFT calculations for this series of molecules.

Recent investigations have shown that the density functional theory (DFT) method provides accurate predictions of structural parameters[23] and nearly quantitative ^{13}C–^{13}C and ^{13}C–^{1}H spin couplings in a wide range of bonding environments without the need for scaling.[24] Also Serianni and co-workers have shown that the B_3LYP method is a suitable method for predicting coupling constants in disaccharides.[25] Consequently, the coupling constants in rutinose, Figure 6, were obtained by finite-field (Fermi contact) double perturbation theory[26] calculated at the B_3LYP/6-311G** level. Appropriate values for the perturbing fields imposed on the coupled nuclei were chosen to ensure sufficient numerical precision, while still allowing a satisfactory low-order finite-difference representation of the effect of the perturbation. Only the Fermi contact component of each coupling constant was considered due to the dominant relationship of this term in J values involving carbon and hydrogen, especially in saturated systems.

All the equations describing the dependencies of $^{2}J_{H-H}$, $^{3}J_{H-H}$, and $^{1}J_{C-H}$ on ω, θ, and φ were parameterized from the calculated

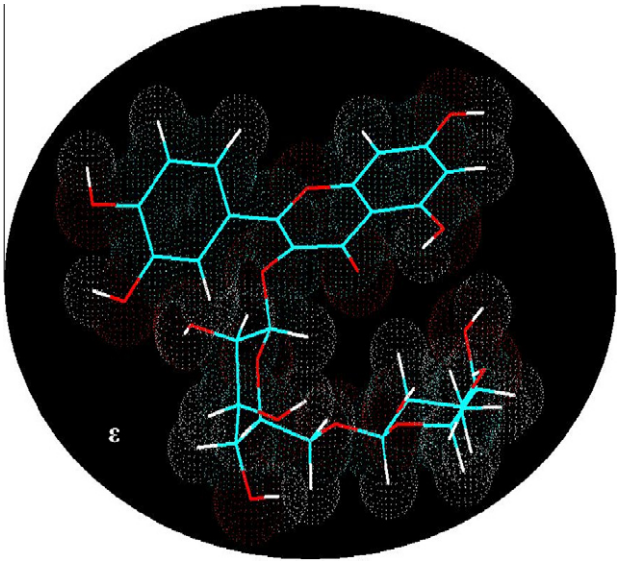

Figure 5. Optimized structure of rutin at the $B_3LYP/6\text{-}311G^{**}$ level in DMSO solvent.

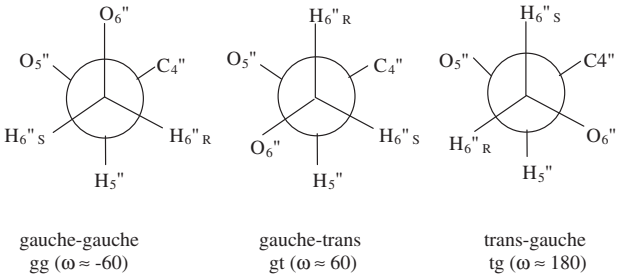

Scheme 1. Idealized rotamers about the C5″–C6″ bond of aldohexopyranosyl rings.

Table 1
Some structural details of rutin's optimized structure at $B_3LYP/6\text{-}311G^{**}$ level

Bond distance (Å)	
O1–C2	1.36
C2–C3	1.33
C2–C1′	1.49
C1′–C2′	1.38
C5″–C6″	1.51
C5″–O5″	1.38
C5″–O6″	1.41
C1‴–O6″	1.39
C1‴–C2‴	1.51
Bond angles (°)	
C2–C1′–C2′	122.0
C2–C3–O	120.0
C3–O–C1″	120.8
C5″–C6″–O6″	113.1
C6″–O6″–C1‴	116.2
Dihedral angles (°)	
O1–C2–C1′–C2′	142.0
C3–C2–C1′–C2′	−43.25
C2–C3–O–C1″	125.2
C5″–C6″–O6″–C1‴	173.0

couplings using the least-squares procedure. Specific staggered hydroxymethyl rotamers of rutinose generated by systematically rotating the (ω = O5″–C5″–C6″–O6″) and (θ = C5″–C6″–O6″–H) torsions, from 0° to 360° in 30° increments by holding both torsion

Table 2
Representation of some experimental and theoretical chemical shifts (ppm) and spin–spin coupling constants (Hz) of rutin in DMSO at 298 K

Chemical shifts						Coupling constant (Hz)	
^1H	Calcd	Exptl	^{13}C	Calcd	Exptl	Exptl	
6	6.25	6.19	2	102.4	99.5	$^3J_{H1'',H2''}$	8.1
8	6.12	6.38	3	97.5	94.4	$^3J_{H2'',H3''}$	9.2
6′	7.10	7.54	4	125.3	122.4	$^3J_{H3'',H4''}$	9.2
5′	6.35	6.84	1′	120.1	117.1	$^3J_{H4'',H5''}$	9.7
2′	7.12	7.53	2′	119.5	116.0	$^3J_{H5'',H6''R}$	2.3
1″	5.80	5.33	1″	105.3	102.0	$^3J_{H5'',H6''S}$	2.3
2″	4.18	3.25	2″	76.7	74.9	$^2J_{H6''R,H6''S}$	−11.7
3″	3.88	3.19	3″	75.3	77.3		
4″	3.51	3.41	4″	72.1	70.9		
5″	3.82	3.28	5″	75.3	76.7		
6″(H_R,H_S)	3.87	3.70	6″	69.2	67.8	$^1J_{C1''',H1'''}$	165.5
1‴	3.48	4.38	1‴	102.3	101.6	$^1J_{C4'',H4''}$	145.5
2‴	3.22	3.26	2‴	72.6	71.4	$^1J_{C5'',H5''}$	141.7
3‴	2.99	3.07	3‴	72.1	71.2	$^1J_{C6'',H6''R}$	142.32
4‴	3.14	3.06	4‴	75.5	72.7	$^1J_{C6'',H6''S}$	143.75
5‴	2.85	3.16	5‴	68.2	69.0		
CH_3	1.28	1.0	CH_3	16.71	18.6		

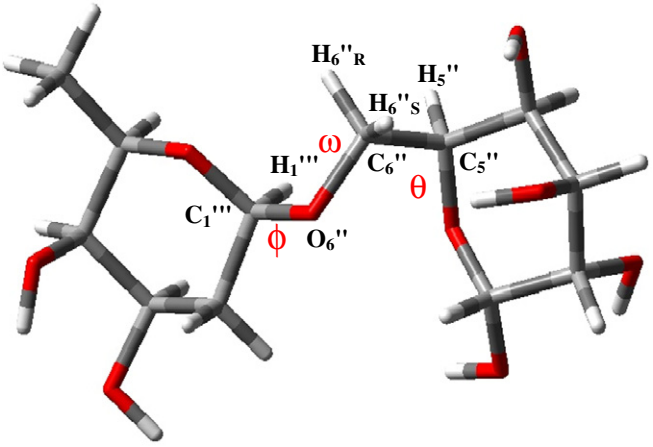

Figure 6. The tube model of rutinose structure to calculate coupling constants that are sensitive to ω, θ, and φ.

angles at fixed values, were constructed in the GAUSSIAN viewer and subsequently geometrically optimized using $B_3LYP/6\text{-}311G^{**}$. These structures were reoptimized taking solvent effects into account.

4.3. Vicinal (three-bond) ^1H–^1H spin–spin coupling constants

The previous study shows two $^3J_{HH}$ values, $^3J_{H5,H6R}$ and $^3J_{H5,H6S}$, in some aldohexopyranoside derivatives that are sensitive to ω.[27]

$^3J_{H5'',H6''R}$ and $^3J_{H5'',H6''S}$ (Eqs. 1 and 2) were computed for rutinose using the set of staggered and eclipsed geometries (Table 3). Karplus equations were also derived by including the effect of θ, but this processing did not improve the quality of Eqs. 1 and 2 significantly. So two $^3J_{HH}$ values, $^3J_{H5'',H6''R}$ and $^3J_{H5'',H6''S}$, are sensitive to ω:

$$^3J_{H5'',H6''R} = 5.07 + 0.49\cos(\omega) + 0.88\sin(\omega) - 0.15\cos(2\omega) + 4.65\sin(2\omega) \quad (\text{rms} = 0.27\ \text{Hz}) \tag{1}$$

$$^3J_{H5'',H6''S} = 4.86 - 1.31\cos(\omega) + 0.07\sin(\omega) + 4.52\cos(2\omega) + 0.06\sin(2\omega) \quad (\text{rms} = 0.18\ \text{Hz}) \tag{2}$$

Figure 7 shows a plot of theoretical $^3J_{H5,H6R}$ and $^3J_{H5,H6S}$ values versus ω, using Eqs. 1 and 2.

Table 3
Torsion angles, ω and θ (°), and calculated $^{2}J_{H6R,H6S}$, $^{3}J_{H5,H6R}$, $^{3}J_{H5,H6S}$, and $^{1}J_{C5,H5}$ values (Hz)

ω (°)	θ (°)	$^{2}J_{H6''R,H6''S}$	$^{3}J_{H5'',H6''R}$	$^{3}J_{H5'',H6''S}$	$^{1}J_{C5'',H5''}$	$C_{5''}$–$C_{6''}$ Rotamer
62	57	−12.5	10.6	1.8	137	
57	−48	−11.2	10.6	2.7	141	*gt*
72	192	−8.7	9.5	1.2	141	
−58	50	−11.6	1.0	2.7	140	
−70	−72	−13.2	1.7	1.6	137	*gg*
−72	171	−8.5	2.4	1.7	137	
176	74	−12.1	4.9	11.0	143	
177	−69	−12.0	4.0	11.3	137	*tg*
176	176	−7.1	4.6	11.0	141	
120	60	−12.9	1.0	3.4	140	
120	−60	−12.8	1.2	2.9	141	
120	180	−8.6	1.0	3.1	145	
0	60	−11.7	6.0	7.7	140	
0	−60	11.7	5.0	8.7	141	
0	180	−7.3	5.3	8.5	140	
−120	60	−13.8	8.6	2.6	141	
−120	−60	−13.6	7.5	3.5	140	
−120	180	−9.3	8.2	2.8	140	

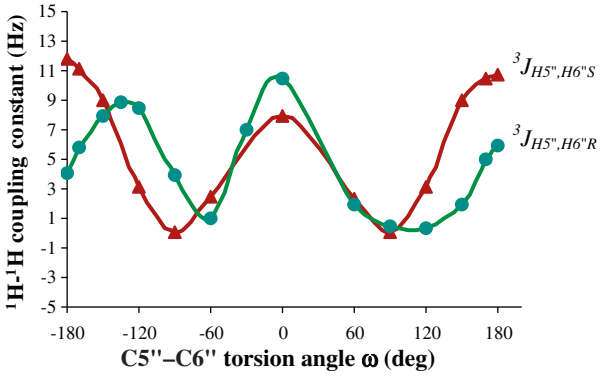

Figure 7. Plots of the dependencies of calculated $^{3}J_{H5'',H6''S}$ and $^{3}J_{H''5,H''6R}$ in rutinose on the ω angle.

4.4. Geminal (two-bond) ^{1}H–^{1}H spin–spin coupling constants

$^{2}J_{H6R,H6S}$ is affected by both ω and θ, but its dependence on θ is significantly greater than its dependence on ω. The latter conclusion is supported by previous studies of Serianni and co-workers,[28] which show that the computed $^{2}J_{H6R,H6S}$ is related to both ω and θ. The additional hyper surface dataset obtained in this work yielded an improved equation (Eq. 3) with substantially smaller rms error. According to the data in Table 3 Eq. 3 relates $^{2}J_{H6''R,H6''S}$ for rutinose to ω and θ:

$$^{2}J_{H6''R,H6''S} = -11.02 + 0.32\cos(\omega) - 2.22\cos(\theta) \quad (\text{rms} = 0.22\ \text{Hz}) \tag{3}$$

The results of the previous study[29] show that the $^{2}J_{HH}$ values in an unsubstituted CH_2OH fragment are influenced by both ω and θ, which could be caused by the value of the H–C–H bond angle (this angle appears relatively constant despite changes in ω and θ) on $^{2}J_{HH}$. So $^{2}J_{HH}$ values in an unsubstituted CH_2OH fragment appear to be influenced minimally by the H–C–H bond angle, but O-substitution affects the H–C–H bond angle significantly. Therefore, this factor may need to be considered in the structural interpretation of $^{2}J_{HH}$.

4.5. One-bond ^{13}C–^{1}H spin–spin coupling constants

C–H bond length is a key determinant of the $^{1}J_{CH}$ value, with shorter bond (greater s-character) yielding larger couplings.[30] Several structural factors influence C–H bond length: axial versus equatorial bond orientation, vicinal lone-pair effects,[30,31] 1,3-lone-pair effect,[32] and 1,4-lone-pair effects.[28] The effects of 1,3-interactions with oxygen lone-pairs are observed on r_{C5-H5} and $^{1}J_{C5''-H5''}$; therefore, the orientation of the vicinal lone-pairs on O5″ and the orientation of the C5″–H5″ bond remain fixed in all structures. A plot of calculated $^{1}J_{C5'',H5''}$ versus $r_{C5''-H5''}$ is linear (Fig. 8) indicating that the C–H bond length is highly correlated with the magnitude of $^{1}J_{CH}$, with shorter bonds yielding larger coupling constants. The shortest C6″–H6″ bond, and the largest $^{1}J_{C6''-H6''}$ values, is expected for a C6″–H6″ bond that does not experience a bond-lengthening vicinal (anti) O6″ lone-pair interaction and a bond-shortening 1,3-interaction with an O5″ lone-pair. A plot of calculated $^{1}J_{C6'',H6''}$ versus $r_{C6''-H6''}$ for staggered rotamers is almost linear, too. The above-mentioned results relate the $^{1}J_{CH}$ to only two torsion angles ω and θ. Rotation of the C6″–O6″ bond modulates the stereoelectronic effect of the O6″ lone-pairs on the C6″–H6″*R* and C6″–H6″*S* bond lengths, but other effects (1,3-lone-pair interactions with O5″ and bond orientation) also influence these bond lengths, so the Karplus equations for rutinose that relate $^{1}J_{C5''-H5''}$ and $^{1}J_{C6''-H6''}$ to ω and θ give relatively large rms errors.

One of the major practical advantages of the angular dependences of $^{1}J_{C,H}$ values is the possibility of determination of the glycosidic-bond torsional angles. The dependencies of $^{1}J_{C1''',H1'''}$ on φ are examined by systematic rotations about φ in rutinose by 10 increments. Computed values of $^{1}J_{C1''',H1'''}$ in optimized structures after every increase in φ dihedral angles are shown in Table 4.

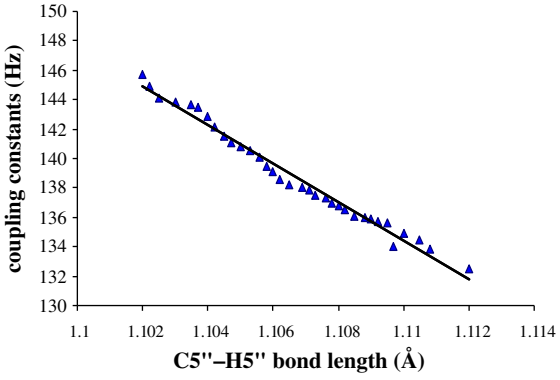

Figure 8. Computed $^{1}J_{C5''H5''}$ versus C5″–H5″ bond lengths. Data were generated from systematic rotations about ω and θ.

Table 4
Effect of torsion angle φ on the computed $^{1}J_{C1''',H1'''}$ (Hz) in rutinose

φ	$^{1}J_{C1''',H'''1'''}$
0	156.6
30	158.7
60	162.1
90	163.1
120	159.3
150	158.1
180	162.2
210	163.5
240	160.2
270	157.5
300	161.3
330	162.5
360	160.8

Table 5
Part (A): Limiting values for $^3J_{H5''H6''R}$ and $^3J_{H5''H6''S}$ in three staggered rotamers about the C5″–C6″ bond in rutinose, Part (B): C5″–C6″ rotamer distribution in rutinose from $^3J_{H5''H6''R}$ and $^3J_{H5''H6''S}$ values and limiting coupling constants in part (A)

Coupling (Hz)	$^3J_{H5H6R}$					$^3J_{H5H6S}$		
	gt	*gg*	*tg*			*gt*	*gg*	*tg*
Part (A)	9.7	1	4.3			1.5	1.4	10.5
				rotamer distribution				
				%*gt*	%*gg*	%*tg*		
Part (B)				36	60	4		

The relationship between $^1J_{C1''',H1'''}$ and φ was parameterized using a complete dataset of 36 data points, yielding Eq. 4, which indicates conformational dependence of coupling constant upon the dihedral angle φ. Also Table 5 shows some experimental coupling constants:

$$^1J_{C1,H1} = 0.57\cos(\varphi) - 2.97\cos(\varphi) + 1.73\sin(\varphi) - 1.59\sin(\varphi) + 162.13 \quad (\text{rms} = 1.41\ \text{Hz}) \tag{4}$$

5. C5–C6 and C6–O6 rotamer distributions in rutinose

Rotameric distributions around the C5″–C6″ and C6″–O6″ bonds of the aldohexopyranosyl ring of rutinose can be determined from $^3J_{H5'',H6''R}$ and $^3J_{H5'',H6''S}$. The limiting values of these couplings depend on assumptions made about the torsion angles and the choice of Karplus equation. The limiting couplings in Table 5 were used to estimate the percentages of C″5–C″6 and C″6–O″6 rotamers in rutinose. According to Table 5 small percentages of *tg* rotamer are observed. Percentages of *gt*, *gg*, and *tg* rotamers were calculated by solving the following three equations simultaneously:

$$^3J_{H5,H6R} = P_{gt}(^3J_{H5,H6R(gt)}) + P_{gg}(^3J_{H5,H6R(gg)}) + P_{tg}(^3J_{H5,H6R(tg)}),$$
$$^3J_{H5,H6S} = P_{gt}(^3J_{H5,H6S(gt)}) + P_{gg}(^3J_{H5,H6S(gg)}) + P_{tg}(^3J_{H5,H6S(tg)}),$$
$$\text{and } P_{gt} + P_{gg} + P_{tg} = 1.$$

In these equations, P is the fraction of the respective rotamer, $^3J_{H5,H6R(gt)}$ is the standard value of $^3J_{H5,H6R}$ in the gt rotamer, $^3J_{H5,H6R(gg)}$ is the standard value of $^3J_{H5,H6R}$ in the *gg* rotamer, and so forth. Standard couplings used in the calculations were derived from Eqs. 1 and 2. It is important to appreciate that substitution at O6″ eliminates O6″–H, thereby preventing the measurement of $^3J_{HCOH}$,[33] which can be used to evaluate the C–O torsion. In this situation, knowledge of the relationships between $^3J_{HH}$, $^2J_{HH}$, and θ can be especially useful.

6. Conclusions

Conformational studies of the exocyclic hydroxymethyl group in the disaccharide rutinose in rutin have relied heavily on the use of $^3J_{HH}$ values to estimate rotamer populations in solution. The strategy was to obtain experimental results from extracted rutin, and then these data were used to test the ability of the DFT methods to estimate the chemical shifts and coupling constants. Good agreement between experimental and theoretical data confirms the accuracy of the B_3LYP/6-311G** method for calculation of chemical shifts and coupling constants of saccharides.

The results show $^3J_{HH}$ values in hydroxymethyl fragments are evaluated mostly by the C–C torsion angle (ω) and less by the C–O torsion angle (θ). Notice that the $^2J_{HH}$ is determined mainly by the C–O torsion angle (θ) in the absence of a hydroxyl proton on O6, when the hydroxyl group is substituted (for example in a (1→6)-glycosidic linkage).

In addition, this report generates new theoretical treatments for flavonoids with a sugar moiety, which makes the interpretation of saccharide conformational analysis more feasible. These results are expected to be helpful for understanding the conformational details of rutin in solution and will give a clue into the design of the binding of rutin to DNA molecules and different enzymes. The present findings make a significant contribution not only for the studies of rutin but also for the related studies of bioflavonoid with a saccharide moiety.

Acknowledgments

The authors would like to appreciate Professor Hiroshi Sugiyama from Tohoku University for his advice and suggestions for this work. We are grateful to the Ministry of Science, Research and Technology, for financial support. Also, we thank IDB for providing the grant for purchasing the 500-MHz NMR instrument.

References

1. Aron, P. M.; Kennedy, J. A. *Mol. Nutr. Food Res.* **2008**, *52*, 79–104.
2. Halliwell, B. *Cardiovasc. Res.* **2007**, *73*, 341–347.
3. Manach, C.; Mazur, A.; Scalbert, A. *Curr. Opin. Lipidol.* **2005**, *16*, 77–84.
4. Chen, Y. T.; Zheng, R. L.; Jia, Z. J.; Ju, Y. *Free Radical Biol. Med.* **1990**, *9*, 19–21.
5. Sun, W. Q.; Sheng, J. F. *Handbook of Natural Active Constituents*; Chinese Medicinal Science and Technology Press: Beijing, 1998; pp 2241–2316.
6. Reynolds, J. E. F. MARTINDALE, The extra pharmacopoeia, 31st ed.; The Royal Pharmaceutical Society, Council of the Royal Pharmaceutical Society of Great Britain: London, 1996; pp 1652–1680.
7. Casley-Smith, J. R.; Morgan, R. G.; Pillar, N. B.; Engl, N. *J. Med. Chem.* **1993**, *329*, 1158–1163.
8. Chen, G.; Zhang, J. X.; Ye, J. N. *J. Chromatogr., A* **2001**, *923*, 255–262.
9. Namazian, M.; Zare, H. R.; Coote, M. L. *Biophys. Chem.* **2008**, *132*, 64–68.
10. Ishii, K.; Furuta, T.; Kasuya, Y. *J. Chromatogr., B: Anal. Technol. Biomed. Life Sci.* **2001**, *759*, 161–168.
11. Song, Z. H.; Hou, S. *Talanta* **2002**, *57*, 59–67.
12. He, J. L.; Yang, Y.; Yang, X.; Liu, Y. L.; Liu, Z. H.; Shen, G. L.; Yu, R. Q. *Sens. Actuators, B* **2006**, *114*, 94–100.
13. Hassan, H. N. A.; Barsoum, B. N.; Habib, I. H. I. J. *Pharm. Biomed. Anal.* **1999**, *20*, 315–320.
14. Legnerova, Z.; Satinsky, D.; Solich, P. *Anal. Chim. Acta* **2003**, *497*, 165–174.
15. Wan, C.; Cui, M.; Song, F.; Liu, Z.; Liu, S. *Int. J. Mass Spectrom.* **2009**, *283*, 48–55.
16. Ray, A.; Kumar, G. S.; Das, S.; Maiti, M. *Biochemistry* **1999**, *38*, 6239–6247.
17. Chowdhury, A. R.; Sharma, S.; Mandal, S.; Goswami, A.; Mukhopadhyay, S.; Majumder, H. K. *Biochem. J.* **2002**, *366*, 653–661.
18. Lallemand, J. Y.; Duteil, M. *Org. Magn. Reson.* **2005**, *9*, 179–180.
19. Frisch, M. J.; Trucks, G. W.; Schlegel, H. B.; Scuseria, G. E.; Robb, M. A.; Cheeseman, J. R.; Zakrzewski, V. G.; Montgomery, J. A.; Stratmann, R. E.; Burant, J. C.; Dapprich, S.; Millam, J. M.; Daniels, A. D.; Kudin, K. N.; Strain, M. C.; Farkas, O.; Tomasi, J.; Barone, V.; Cossi, M.; Cammi, R.; Mennucci, B.; Pomelli, C.; Adamo, C.; Clifford, S.; Ochterski, J.; Petersson, G. A.; Ayala, P. Y.; Cui, Q.; Morokuma, K.; Malick, D. K.; Rabuck, A. D.; Raghavachari, K.; Foresman, J. B.; cioslowski, J.; Ortiz, J. V.; Stefanov, B. B.; Liu, G.; Liashenko, A.; Piskorz, P.; Komaromi, I.; Gomperts, R.; Martin, R. L.; Fox, D. J.; Keith, T.; Al-Laham, M. A.; Peng, C. Y.; Nanayakkara, A.; Ghonzalez, C. V.; Challacombe, M.; Gill, P. M. W.; Johnson, B. G.; Chen, W.; Wong, M.; Andres, J. L.; Head-Gordon, M.; Replogle E. S.; Pople, J .A. *GAUSSIAN 2003 (Revision-B)*, Gaussian, Inc.: Pittsburgh PA, 2003.
20. Parr, R. G.; Yang, W. *Density-Functional Theory of Atoms and Molecules*; Oxford University Press: Oxford, 1989.
21. Cossi, M.; Barone, V.; Cammi, R.; Tomasi, J. *Chem. Phys. Lett.* **1996**, *255*, 327–335.
22. Wolinski, K.; Hilton, J. F.; Pulay, P. *J. Am. Chem. Soc.* **1990**, *112*, 8251–8260.
23. Bauschlicher, C. W., Jr.; Partridge, H. *Chem. Phys. Lett.* **1995**, *240*, 533–540.
24. Cloran, F.; Carmichael, I.; Serianni, A. S. *J. Phys. Chem. A* **1999**, *103*, 3783–3795.
25. Cloran, F.; Carmichael, I.; Serianni, A. S. *J. Am. Chem. Soc.* **1999**, *121*. 9851-9851.
26. Kowalewski, J.; Laaksonen, A.; Root, B.; Siegbahn, P. *J. Chem. Phys.* **1979**, *71*, 2896–2902.
27. Tafazzoli, M.; Ghiasi, M. *Carbohydr. Res.* **2007**, *342*, 2086–2096.
28. Stenutz, R.; Carmichael, I.; Widmalm, G.; Serianni, A. S. *J. Org. Chem.* **2002**, *67*, 949–958.
29. Serianni, A. S.; Wu, J.; Carmichael, I. *J. Am. Chem. Soc.* **1995**, *117*, 8645–8650.
30. Podlasek, C. A.; Stripe, W. A.; Carmichael, I.; Shang, M.; Basu, B.; Serianni, A. S. *J. Am. Chem. Soc.* **1996**, *118*, 1413–1425.
31. Kennedy, J.; Wu, J.; Drew, K.; Carmichael, I.; Serianni, A. S. *J. Am. Chem. Soc.* **1997**, *119*. 8933-6448.
32. Cloran, F.; Zhu, Y.; Osborn, J.; Carmichael, I.; Serianni, A. S. *J. Am. Chem. Soc.* **2000**, *122*, 6435–6448.
33. Fraser, R. R.; Kaufman, M.; Morand, P.; Govil, G. *Can. J. Chem.* **1969**, *47*, 403–409.